COMPUTER MODELLING OF HEAT AND MASS FLOW IN WARM GROUND, KARAPITI

J. NEWSON & M. J. O'SULLIVAN

Dept of Engineering Science, The University Of Auckland.

SUMMARY – Heat and mass transfer in warm soil at Karapiti have been modelled using the TOUGH2 geothermal simulator. A range of van Genuchten parameters has been identified for modelling the unsaturated zone processes at this site, Shallow (0 – 20 cm) steady temperature and gas saturation for depth profiles are well matched. The propagation of the diurnal temperature wave into the soil has been successfully modelled, and this process has quantified heat and mass flows through the soil.

1 INTRODUCTION

This study follows on from field data collection (Bromley & Hochstein, 2001), and analytic modelling of heat and mass flows through warm soil at Karapiti (Newson, et al, 2001).

One problem with the analytic methods used for the 2001 study is that only single phase flow can be considered, whereas at some sites a steam/water mixture may coexist with air in the shallow unsaturated ground. For this study the geothermal simulator TOUGH2 (Pruess, 1991)is used to model heat and mass transfer in saturated or unsaturated, warm, ground.

Four data sets are used to calibrate the model: two steady state data sets Consisting of temperature and gas saturation versus depth profiles; and two sets of transient data, which are the amplitude decay and phase shift of the diurnal temperature wave as it travels into the soil.

The resulting model gives us information on a variety of soil properties and heat and mass flows. It indicates a suitable range of parameters for the van Genuchten-Mualem relative permeability and van Genuchten capillary functions (Mualem, 1976; van Genuchten, 1980) lambda, alpha, residual saturation, and maximum capillary pressure, and also gives values for mass and heat flow, and wet and dry thermal conductivity at the site.

2 BACKGROUND

2.1 Calibration data

Field measurements

Air temperature, and ground temperature at depths of 1, 5, 10, 15, and 20 cm were measured at 6 sites at Karapiti, in the summer of 2000 by Bromley and Hochstein (Bromley and Hochstein, 2001). This data clearly shows the effect of the diurnal air temperature cycle at all the measured depths.

At the same time cores from 0 to 15 cm, and 15 to 30 cm depth were retrieved for laboratory determination of water content and porosity.

This study uses the data from site KP03, which has temperatures of around 40 °C at a depth of 20 cm.

Laboratorv data

The results of the laboratory work enabled calculation of saturation and porosity for the core samples. The gas saturation and porosity for core from KP03 is shown in Table 1:

Table 1. Gas saturation for KP03 core

depth	Gas saturation	Porosity
0 – 15 cm	0.49	0.60
15 – 30 cm	0.37	0.62

For modelling purposes porosity is 0.61, and the saturation values above are considered to be at the midpoint of the cores; ie at 0.075 and 0.225 m depths.

2.2 Modelling background

Mathematical models

Newson, et al, (2001) used three simple analytical mathematical models to investigate mass and heat flows, and soil thermal properties, at the Karapiti sites.

The first model, a purely conductive heat flow model, suggested that KP03 heat flows were 72.3 W/m^2, given a thermal conductivity of 1 W.m/K.

The second model included a heat loss boundary condition, but did not match the measured data and did not yield any useful information.

The third model included mass flow thus allowing advective/conductive heat transfer in the soil. This model predicted a deep upflow with a temperature of 47.7°C.

Conductivity

TOUGH2 has several options relating thermal conductivity to saturation. The option selected for this study has thermal conductivity K as a function of the square root of saturation (Equation (1))

$$K = KDRY + \sqrt{S_l}\,(KWET - KDRY) \qquad (1)$$

Where KWET and **KDRY** are the wet and *dry* thermal conductivity, and are specified in the model input. S_l is the liquid saturation. Equation **(1)** includes porosity implicitly in the measurement or calculation of values of KWET and **KDRY.**

For the present study we calculated a value for KWET and **KDRY** based on the mean value of two permeable media models:

- a parallel plate model of rock and fluid, where the heat flow is parallel to the layers of rock and fluid. The wet and dry thermal conductivities are shown in Equations (2) and (3):

$$KDRY_{PARALLEL} = (1-\varphi)K_{ROCK} + K_{AIR} \qquad (2)$$

$$KWET_{PARALLEL} = (1-\varphi)K_{ROCK} + K_{WATER} \qquad (3)$$

- and a series model, where the heat flow is across layers of rock and fluid. The wet and *dry* thermal conductivities are given in equations **(4)** and *(5)*.

$$1/KDRY_{SERIES} = \varphi/K_{AIR} + (1-\varphi)/K_{ROCK} \qquad (4)$$

$$1/KWET_{SERIES} = \varphi/K_{WATER} + (1-\varphi)/K_{ROCK} \qquad (5)$$

Where ϕ is the porosity, the thermal conductivity of air, water and rock are given in Table 2:

Table **2:** Symbols and values for thermal conductivity.

	air	water	rock
Symbol	K_{AIR}	K_{WATER}	K_{ROCK}
Thermal conductivity (W.m/K)	*0.026*	*0.6*	2.5

The arithmetic mean of the series and parallel models (Equations (6) and (7)) is used to give KWET and **KDRY** for each site, based on laboratory measurements.

$$KWET = \frac{KWET_{SERIES} + KWET_{PARALLEL}}{2} \qquad (6)$$

$$KDRY = \frac{KDRY_{SERIES} + KDRY_{PARALLEL}}{2} \qquad (7)$$

KWET and **KDRY** are then averaged for all the sites, and the resulting ratio of KWET:KDRY (2.48:1) is used in this study. This procedure eliminates one parameter from the model fitting process.

3 COMPUTER MODEL

3.1 Simulator

The geothermal simulator TOUGH2 has been used for all the simulations described in this paper. TOUGH2 can model the transport of energy, water, steam, air and water vapour through porous media. These capabilities are required for modelling the unsaturated zone above the water table.

TOUGH2 allows a choice of relative permeability and capillary functions. After some experimentation, for this study the van Genuchten-Mualem relative permeability function, and the van Genuchten capillary function were selected because they are widely used in unsaturated zone modelling.

3.2 Model grid

The model grid is a **1** m **x 1** m vertical column, divided into 35 layers. The layer structure is very fine at the top of the model to provide the definition required to match the field data. The layer thickness increases with depth; the lowest layer, at 50 m depth, is 5 m thick. The top block of the model is connected to a very large 'atmosphere' block, which is large enough for specified atmospheric conditions to remain unchanged despite flows into and out of the model.

3.3 Model input and boundaries

The permeability **is** 10^{-13} m^2, and the porosity is 0.61. The model has very low sensitivity with respect to permeability and porosity; and these parameters were not varied for model calibration.

The side boundaries of the model are closed. The top boundary is open to an 'atmosphere' block, and there is a specified heat and mass input to the base of the model. The atmospheric temperature is derived from the Fourier analysis of the measured data, and a humidity of 85 % is used.

3.4 Calibration parameters

The thermal conductivity is discussed in Section **2.2.** The mass flow (and an associated enthalpy) and heat flow are specified as input to the base of the model, which provides the heat and mass upflows through the model.

The van Genuchten equations relate relative permeability (Equations (8) and (9)) and capillary pressure (Equations (10) and **(11)**) to saturation. The form the equations take in TOUGH2 is:

$$k_{rl} = \begin{cases} \sqrt{S^*}\left\{1-\left(1-[S^*]^{1/\lambda}\right)^{\lambda}\right\}^2 & \text{if } S_l < S_{ls} \\ 1 & \text{if } S_l \geq S_{ls} \end{cases} \qquad (8)$$

$$k_{rg} = 1 - k_{rl} \qquad (9)$$

$$P_{cap} = -P_0\left(\left[S^*\right]^{-1/\lambda} - 1\right)^{1-\lambda} \quad (10)$$

subject to

$$-P_{max} \le P_{cap} \le 0 \quad (11)$$

where

$$S^* = (S_l - S_{lr})/(S_{ls} - S_{lr}) \quad (12)$$

k_{rl} is the relative permeability to liquid; and

k_{rg} is the relative permeability to gas.

P_{cap} is the capillary pressure

The fully mobile liquid saturation and the residual gas saturation are set equal to 1.0 and 0.0 respectively. The parameters required for the TOUGH2 model calibration are given in Table 3.

Table 3. Input parameters for calibration of TOUGH2 model.

Parameter name	Symbol	Unit
Lambda	λ	
Residual saturation	S_{lr}	
Fully mobile liquid saturation	S_{ls}	
Residual gas saturation	S_{gr}	
Maximum capillary suction	P_{max}	Pa
Alpha	α	1/Pa
Mass flow	q_m	kg/s
Enthalpy of the mass flow	h	(J/kg)
Heat flow	q_e	W
Saturated thermal conductivity	KWET	W.m/K
(KWET=2.48KDRY)		
Dry thermal conductivity	KDRY	W.m/K

3.5 Calibration data for modelling

From the Fourier analysis of the field measurements, and the laboratory data, we have the following calibration data for modelling soil properties and shallow heat and mass transfer.

1. Steady state data which consists of
   - the stable, or average, temperature profile with depth, and;
   - two saturation values at 0.075 m and 0.225 m depth.
2. Transient data for:
   - the amplitude decay of the temperature wave with depth, and;
   - phase shift of the temperature wave with depth.

3.6 Calibration process

The steady model output for temperature is matched to the calibration data by adjusting the heat and mass input. At this stage the saturation vs depth results are not expected to be a good match. A series of simulations are then performed for a range of van Genuchten parameters, and the model results for saturation versus depth are tested for fit to the calibration data using a simple objective function (the sum of squares of the difference between the model results and calibration data).

Once the set of van Genuchten parameters which optimises the saturation versus depth profile of the model is identified, they are used in the model input, and the mass input and the heat input are varied to recalibrate the steady model. Provided that the changes in mass and heat input are not too great there is little change in the saturation versus depth model profile. This process optimises the model fit for temperature and saturation versus depth.

At this point we have a model which is calibrated for the steady state. If the mass input, heat input, and thermal conductivities are all increased or decreased in the same proportion, there is little change in the steady state results (for this study the proportion has a range of 0.8 to 1.1). This characteristic is important for calibration of the transient model.

The transient simulation imposes the daily sinusoidal temperature variation, also from the Fourier analysis, to the atmosphere block. The simulation is run for 5 cycles (5 days), ensuring a stable cycle at all depths in the model. The resulting amplitude decay and phase shift of the model output with depth are compared with the calibration data.

The amplitude and phase behaviour of the temperature wave is strongly dependent on the mass and heat flow. Hence the calibration for the transient model is achieved by running a series of simulations, each of which has a steady state and a transient run. For each simulation, the mass input, heat input, and thermal conductivities are increased or decreased in the same proportion. This retains the steady state results for all the simulations, while changing the temperature amplitude and phase behaviour of the transient run. Finding the optimal mass flow for the model is relatively simple, because the fit of the amplitude decay to calibration data is inversely related to the fit of the phase shift. The model parameters are optimised when the objective function for amplitude decay is equal to the objective function for the phase shift.

4 RESULTS

4.1 Steady state model: van Genuchten parameters

The model is initially calibrated for temperature by varying the heat and mass input independently, then four sets of simulations are run, one for each van Genuchten parameter. In each set, one parameter is varied over a range of values. Variation of the van Genuchten parameters has **only** a small effect on the temperature profile; Figure 1 shows the temperature versus depth model results for lambda = 0.5 to lambda = 0.9. The temperature difference is around 1°C at 20 cm depth over the given range of lambda, which is typical of the temperature versus depth results from all sets of simulations.

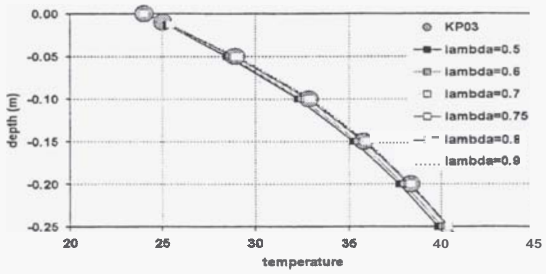

Figure 1. Temperature vs depth profile showing calibration data (large dots) and model results for lambda values from 0.5 to **0.9.**

In contrast, the van Genuchten parameters have a large effect on gas saturation. Figure **2,** Figure **3,** Figure **4,** and Figure 5 show the model results for variation of lambda, alpha, residual saturation, and maximum capillary pressure, respectively, and show that variation of any of these four van Genuchten parameters cause significant changes to the gas saturation profile with depth.

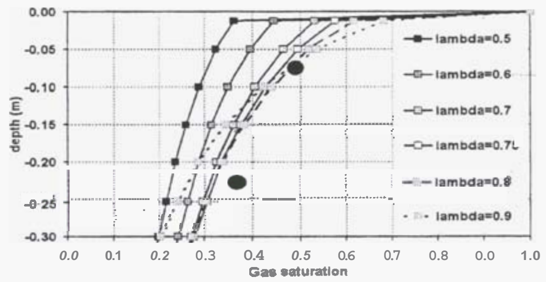

Figure **2.** Saturation vs depth profile showing calibration data (large dots) and model results for lambda values from 0.5 to 0.9.

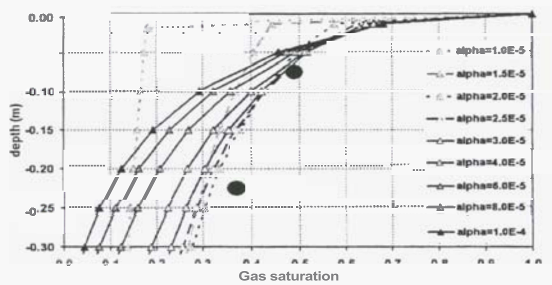

Figure **3.** Saturation vs depth profile showing calibration data (large dots) and model results for alpha values from 1.0E-5 to 1.0E-4 1/Pa.

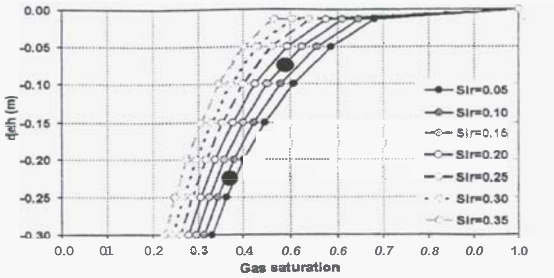

Figure **4.** Saturation vs depth profile showing calibration data (large dots) and model results for residual saturation from 0.05 to 0.35.

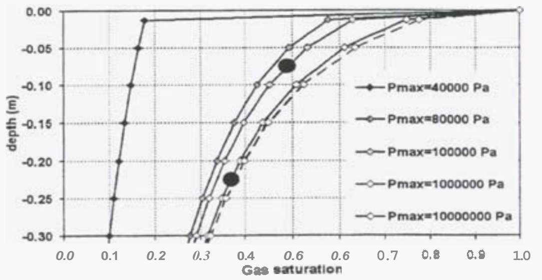

Figure 5. Saturation vs depth profile showing calibration data (large dots) and model results for maximum capillary pressure from 0.4bar to 100 bar.

Because the van Genuchten parameters are significant when calibrating gas saturation, and are a minor influence on temperature, the objective functions for gas saturation only are shown in Figure 6, Figure **7,** Figure 8, and Figure 9. This approach can be expected to indicate a range of appropriate parameter values rather than an exact figure.

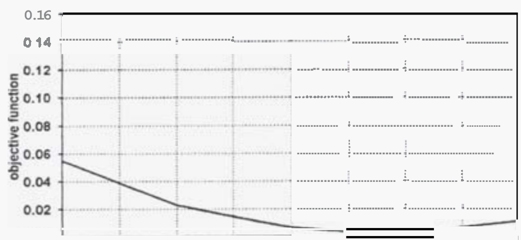

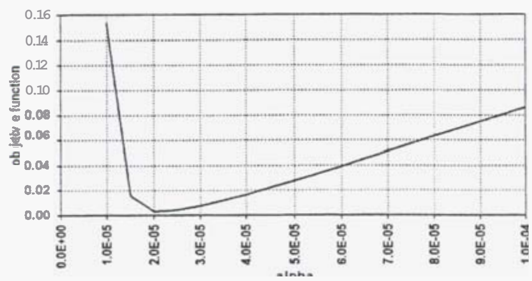

Figure **7.** Objective function for saturation, showing sensitivity to alpha.

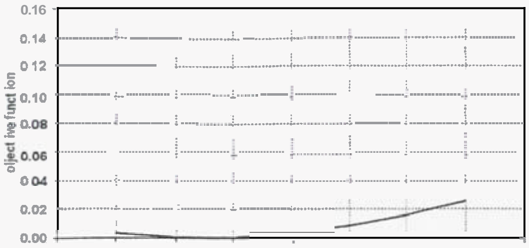

Figure 8. Objective function for saturation showing sensitivity to residual saturation.

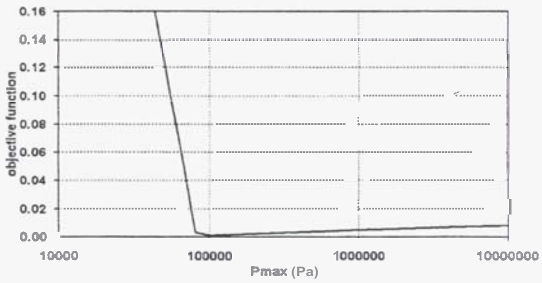

Figure 9. Objective function for saturation showing sensitivity to maximum capillary pressure.

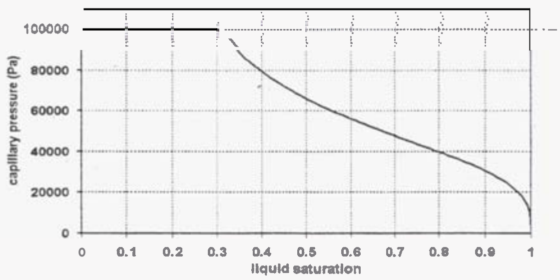

Figure 10 The TOUGH2 capillary function for the van Genuchten parameters in Table **4.**

4.2 Steady state model: mass and heat flow

The model with the final choice of van Genuchten parameters, is then re-calibrated by varying mass and heat flow, although the changes are relatively minor because the effect of van Genuchten parameters on temperature is not large.

The resulting temperature and saturation profiles are given in Figure 11, and Figure **12,** respectively.

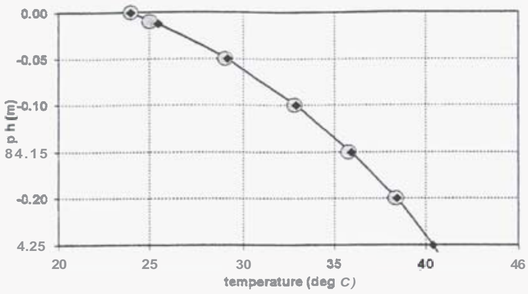

Figure 11. Temperature **vs** depth profile: calibration data (large dots), and best fit steady state model results (line with diamonds).

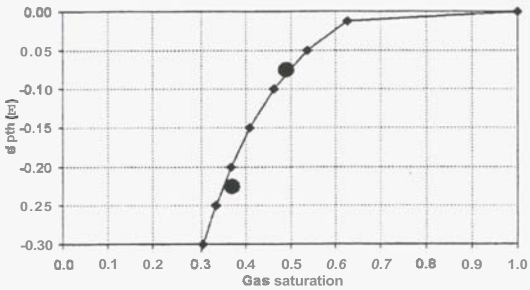

Figure **12.** Saturation **vs** depth profile: calibration data (large dots), and best fit steady state model results (line with diamonds).

4.3 Transient model: Optimum mass flow

The steady state model described above provides the initial conditions, and initial parameters, for one of the transient simulations. **A** series of simulations are run as described in Section 3.6; this allows the steady state results to be maintained. However, the transient model results for different mass input (and proportional heat input and conductivity parameters – see Section 3.6) show significant differences: for increasing mass flows through the model, the match to temperature wave amplitude decay with depth improves, while the inverse is true for phase shift with depth (Figure 13). The best match for both is at the cross-over point, in this case at around a mass input of 0.000816 kg/s. The corresponding heat flow, KWET, and KDRY are given in Table **4.**

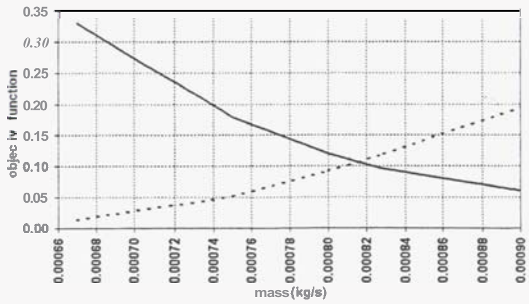

Figure **13.** Objective functions for the transient model results: phase **shift** (dotted line), and amplitude decay (solid line).

Table **4.** Parameters for the best fit model to all the calibration data.

Parameter	Estimate
Lambda	0.7
Alpha	**2.0E-5**
Residual saturation	**0.15**
Max. capillary pressure	**100000**
Mass flow	0.000816 kg/s/m^2
Heat flow	**170.81** W/m^2
KWET	**0.927** W.m/K
KDRY	**0.374** W.m/K

Figure 14 and Figure 15 show the calibration data, and model results using the parameters in Table 4, for amplitude decay and phase shift with depth.

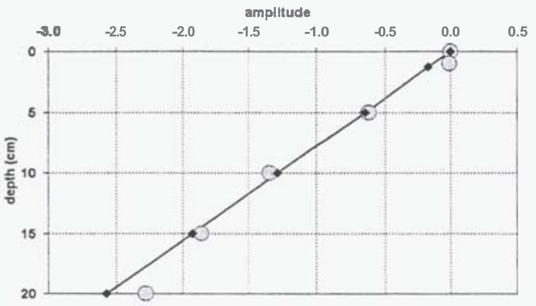

Figure **14.** Amplitude decay with depth of the diurnal temperature wave. Large dots are the calibration data, the line is the model results.

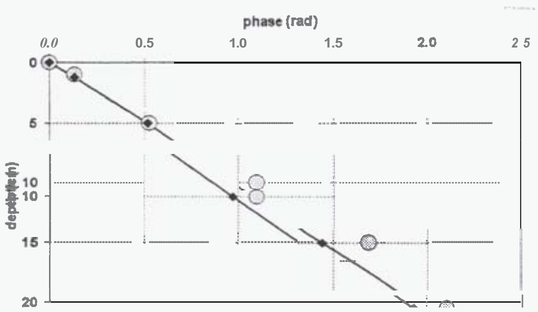

Figure **15.** Phase shift with depth of the diurnal temperature wave. Large dots are the calibration data, the line is the model results.

The match in Figure 14 .is good except at 1 cm depth, however this value in the calibration data is probably a result of surface processes which are not modelled by TOUGH2. Figure 15 shows that the result for phase shift vs depth, is also a reasonable match, particularly in the top section of the profile.

5 DISCUSSION

A simple computer model has been calibrated to fit four data sets. The modelling process demonstrates that the important parameters for modelling the unsaturated zone are the relative permeability and capillary functions, that the behaviour of the diurnal temperature fluctuation with depth is sensitive to the heat and mass flows through the soil.

We have also estimated the van Genuchten parameters for KP03, and quantified mass flow and heat flow through warm ground, at around 0.0008 kg/s/m^2, and 170 W/m^2. A previous simple conductive model (Newson, et al, 2001) indicated heat flows of 72.3 W/m^2; but this study shows that advective heat flow is an important heat transfer process in warm geothermal ground.

5.1 Future work

This study has shown that a very simple computer model can yield useful information about soil properties and heat and mass transfer in warm ground. This also suggests that the calibration process used in this study is successful, and can be applied to data from other sites.

Future work on modelling geothermal soil processes at Karapiti will involve using a similar method to that described for this study, but automating the parameter estimation process by using the inverse modelling program ITOUGH. Other possibilities are to investigate non-homogeneous soil structures, and also the role of diurnal air pressure fluctuations.

6 REFERENCES

Bromley, C. J. & Hochstein, M. P. (2001). Thermal properties of Steaming Ground, Wairakei, New Zealand. ***23rd New Zealand Geothermal Workshop,*** University of Auckland, Auckland, New Zealand.

Mualem, **Y.** (1976). A new model for predicting the hydraulic conductivity of unsaturated porous media. ***Water Resources Research,* 12,** 513-522.

Newson, J., O'Sullivan, M. J., Bromley, C. J. & Hochstein, M. P. (2001). Modelling Shallow Heat Transfer at Karapiti. ***23rd New Zealand Geothermal Workshop,*** University of Auckland, Auckland, New Zealand.

Pruess, **K.** (1991). ***TOUGH2, a general purpose numerical simulator for multiphase fluid and heat flow.*** Lawrence Berkeley Laboratory, CA. LBL-29400.

van Genuchten, M. T. (1980). A closed form equation for predicting the hydraulic conductivity of unsaturated soils. ***Soil Science Society of America Journal,*** 44,892-898.